

Temperature compensation through systems biology

Peter Ruoff¹, Maxim Zakhartsev^{2,*} and Hans V. Westerhoff^{3,4}

1 Department of Mathematics and Natural Science, University of Stavanger, Norway

2 Biochemical Engineering, International University of Bremen, Germany

3 Manchester Centre for Integrative Systems Biology, School for Chemical Engineering and Analytical Sciences, The University of Manchester, UK

4 BioCentre Amsterdam, FALW, Free University, Amsterdam, the Netherlands

Keywords

control coefficients; gene expression; metabolic regulation; systems biology; temperature compensation

Correspondence

P. Ruoff, Department of Mathematics and Natural Science, Faculty of Science and Technology, University of Stavanger, N-4036 Stavanger, Norway
Fax: +47 518 41750
Tel: +47 518 31887
E-mail: peter.ruoff@uis.no
Website: <http://www.ux.uis.no/~ruoff>

*Present address

Department of Marine Animal Physiology, Alfred Wegener Institute for Marine and Polar Research (AWI), Bremerhaven, Germany

(Received 1 October 2006, revised 7 December 2006, accepted 11 December 2006)

doi:10.1111/j.1742-4658.2007.05641.x

Temperature is an environmental factor, which influences most of the chemical processes occurring in living and nonliving systems. Van't Hoff's rule states that reaction rates increase by a factor (the Q_{10}) of two or more when the temperature is increased by 10 °C [1]. Despite this strong influence of temperature on individual reactions, many organisms are able to keep some of their metabolic fluxes at an approximately constant level over an extended temperature range. Examples are the oxygen consumption rates of ectotherms living in costal zones [2] and of fish [3], the period lengths of all circadian [4] and some ultradian [5,6] rhythms, photosynthesis in cold-adapted plants [7,8], homeostasis during fever [9], or the regulation of heat shock proteins [10].

Temperature has a strong influence on most individual biochemical reactions. Despite this, many organisms have the remarkable ability to keep certain physiological fluxes approximately constant over an extended temperature range. In this study, we show how temperature compensation can be considered as a pathway phenomenon rather than the result of a single-enzyme property. Using metabolic control analysis, it is possible to identify reaction networks that exhibit temperature compensation. Because most activation enthalpies are positive, temperature compensation of a flux can occur when certain control coefficients are negative. This can be achieved in networks with branching reactions or if the first irreversible reaction is regulated by a feedback loop. Hierarchical control analysis shows that networks that are dynamic through regulated gene expression or signal transduction may offer additional possibilities to bring the apparent activation enthalpies close to zero and lead to temperature compensation. A calorimetric experiment with yeast provides evidence that such a dynamic temperature adaptation can actually occur.

In 1957, Hastings and Sweeney suggested that in biological clocks such temperature compensation may occur as the result of opposing reactions within the metabolic network [11]. Later kinetic analysis of the problem [12] reached essentially the same conclusion, and predictions of the theory have been tested by experiments using *Neurospora*'s circadian clock [13] and chemical oscillators [14,15].

In this study, we use metabolic and hierarchical control analysis [16–22] to show how certain steady-state fluxes in static reaction networks can be temperature compensated according to a similar principle, and how dynamic networks have an additional repertoire of mechanisms. This study is mostly theoretical, but we use the temperature adaptation of yeast cells and of photosynthesis as illustrations. These and other

systems (e.g. adaptation of gene expression) warrant experimental studies in their own right, which we wish to cover in subsequent work.

Results and Discussion

Global condition for temperature-compensated flux

Here we derive the condition for temperature compensation for a global reaction kinetic network. We refer to this condition as *global*, because the network is assumed to contain *all* biochemical processes (at the genetic and metabolic levels) that occur in the system. Consider a set of N elementary single-step reactions describing a global network. Each reaction i is assigned a rate constant k_i [23] and a steady-state flux (reaction rate) J_i with associated activation enthalpy $E_a^{k_i}$. Here, reversible reactions may be considered as two separate reactions; an alternative is to look upon k_i as a parameter that proportionally affects both the forward and the reverse reaction of the step [23]. Rate constants and absolute temperature are connected via the Arrhenius equation $k_i = A_i e^{-\frac{E_a^{k_i}}{RT}}$, where activation enthalpies $E_a^{k_i}$ are considered to be independent of temperature. The Arrhenius factor A_i subsumes any structural activation entropy. Flux J_j (i.e. the flux of elementary reaction ' j ') becomes temperature compensated within a temperature interval around a reference temperature T_{ref} (at which parameters and rate constants are defined) if the following balancing equation is satisfied (for derivation, see the supplementary Doc. S1):

$$\frac{d \ln J_j}{d \ln T} = \frac{1}{RT} \sum_{i=1}^N {}^*C_i^j E_a^{k_i} = 0 \quad (1a)$$

${}^*C_i^j$ is the global control coefficient [19,21] of flux with respect to the rate constant k_i defined as ${}^*C_i^j = \frac{\partial \ln J_j}{\partial \ln k_i}$. ${}^*C_i^j$ measures the change in flux for a fractional increase in k_i , therein comprising the effects of changes in gene expression or signal transduction that may affect the concentration and activity of the enzyme-catalyzing step. In general, the global control coefficients obey the summation theorem $\sum_{i=1}^N {}^*C_i^j = 1$ [19,21]. Because the activation enthalpies ($E_a^{k_i}$) are positive, temperature compensation is only possible if some of the global control coefficients are negative.

The condition for temperature compensation using metabolic control coefficients

Sometimes a biochemical system is described only at its metabolic level of organization. In this case, one

can use *metabolic* control coefficients, denoted by capital C without the asterisk [19,21], which is a set addressing the control by all the enzymes/steps at the metabolic level and do not include transcriptional, translational processes or signal-transduction events. The effects of these at the metabolic level should be made explicit in terms of changes in the amount or covalent modification state of the enzymes. Accordingly, the 'balancing equation' is given by (see supplementary Doc. S1 for derivation):

$$\frac{d \ln J_j}{d \ln T} = \sum_i C_{k_i^{\text{cat}}}^{J_j} \frac{E_a^{k_i^{\text{cat}}}}{RT} + \sum_m C_{k_m^{\text{cat}}}^{J_j} R_T^{e_m} + \sum_l R_{K_l}^{J_j} \frac{E_a^{K_l}}{RT} = 0 \quad (1b)$$

The first term on the right-hand side of Eqn (1b) describes the contribution of k_i^{cat} (turnover number), where $C_{k_i^{\text{cat}}}^{J_j} = \frac{\partial \ln J_j}{\partial \ln k_i^{\text{cat}}}$ is the *metabolic* control coefficient and $E_a^{k_i^{\text{cat}}}$ is the corresponding activation enthalpy of the turnover number k_i^{cat} . The second term is the contribution due to the variation of the concentration of active enzyme m (e_m) by altered gene expression, translation or signal transduction. It contains the temperature-response coefficient of the activity of that step $R_T^{e_m} \equiv \frac{d \ln e_m}{d \ln T}$. If one is not aware of the change in enzyme activity due to these hierarchical mechanisms, one may measure an apparent activation enthalpy $E_{a,\text{apparent}}^{k_i^{\text{cat}}} = E_a^{k_i^{\text{cat}}} + RT \cdot R_T^{e_m}$. With this Eqn (1b) reduces to:

$$\frac{d \ln J_j}{d \ln T} = \sum_i C_{k_i^{\text{cat}}}^{J_j} \frac{E_{a,\text{apparent}}^{k_i^{\text{cat}}}}{RT} + \sum_l R_{K_l}^{J_j} \frac{E_a^{K_l}}{RT} = 0 \quad (1c)$$

If an increase in temperature leads to a decrease in the expression level of the enzyme-catalyzing step m , the temperature-response coefficient of the enzyme becomes negative. The apparent activation enthalpy of that step in a metabolic network may be zero or have negative values.

The final term in Eqn (1b) describes the contribution due to changes in the rapid equilibria or steady states that the enzyme is engaged in with substrates, inhibitors and activators. For substrates X_l , K_l is the (apparent) Michaelis–Menten constant and $E_a^{K_l}$ is the formation enthalpy ΔH_l^0 associated with K_l [1,24]. $E_a^{K_l}$ tends to be positive, favoring dissociation at higher temperatures [1,24]. $R_{K_l}^{J_j} = \frac{\partial \ln J_j}{\partial \ln k_l}$ is the response coefficient of the flux with respect to an increase in the Michaelis–Menten constant [25].

An example of temperature compensation via and of an enzyme's expression level

In the following example we illustrate the use of global and metabolic control coefficients to obtain tempera-

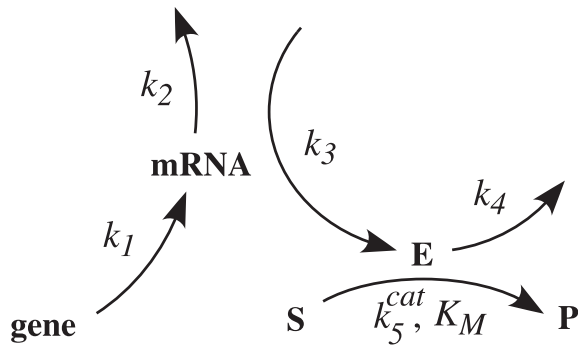


Fig. 1. Simple model of transcription (mRNA synthesis with rate constant k_1) and translation (protein synthesis with rate constant k_2) of an enzyme E , which catalyzes the conversion of $S \rightarrow P$. All reactions are considered to be first-order, except for reaction rate $J_5 = \frac{d[P]}{dt} = \frac{k_5^{cat} e_{ss} [S]}{K_M + [S]}$. The other constants are: k_2 , rate constant for mRNA degradation; k_4 , rate constant of enzyme degradation. K_M and k_5^{cat} are the Michaelis–Menten constant and the turnover number, respectively.

ture compensation in enzyme activity and steady-state level. Figure 1 shows a model of enzyme expression (translation and transcription) in which the enzyme catalyzes the reaction $S \rightarrow P$. For the sake of simplicity, we assume that transcription, translation and the degradation processes have pseudo first-order kinetics with respect to their substrates, i.e. we neglect saturation effects for the RNA polymerase catalyzing transcription, the RNase catalyzing the breakdown of RNA, the ribosomes catalyzing the synthesis of E , and the proteasomes/proteases catalyzing the degradation of E . The steady-state flux (J_5) through step 5 for producing P is described by

$$J_5 = \frac{k_5^{cat} e_{ss} [S]}{K_M + [S]} = \frac{k_1 k_2 k_5^{cat}}{k_2 k_4} \cdot \frac{[S]}{K_M + [S]} \quad (2)$$

where e_{ss} is the steady-state level of E , i.e. the level attained after all processes in the system have relaxed, including those of transcription and translation. The global control coefficients calculated from this equation are $*C_{k_5^{cat}}^{J_5} = 1$ and $*C_{k_i}^{J_5} = 1$ for $i = 1, 3$ and -1 for $i = 2, 4$, whereas the (global) response coefficient with respect to the Michaelis–Menten constant amounts to $*R_{K_M}^{J_5} = \frac{\partial \ln J_5}{\partial \ln K_M} = \frac{K_M}{K_M + [S]}$. Assuming an Arrhenius temperature dependence of rate constants k_i and k_5^{cat} , J_5 can be temperature compensated due to the negative control coefficients of reactions 2 and 4. If the enthalpy of formation of the enzyme substrate complex is negative (which is the more common case), such compensation may also derive from the negative response coefficient.

Likewise, when describing the system at the metabolic level we get $C_{k_5^{cat}}^{J_5} = 1$ and the (metabolic) response coefficient $R_{K_M}^{J_5} = \frac{\partial \ln J_5}{\partial \ln K_M} = \frac{K_M}{K_M + [S]}$. Because $\frac{d \ln J_5}{dT}$ and the

activation and formation enthalpies are unaffected whether the description occurs globally or at a metabolic level, an expression for the temperature variation of the enzyme's steady-state level can be found by comparing the global and metabolic balancing equations (Eqns 1a, 1b)

$$\frac{E_{a,apparent}^{J_5} - E_a^{J_5}}{RT} = \frac{d \ln e_{ss}}{d \ln T} = \frac{1}{RT} (E_a^{k_1} + E_a^{k_3} - E_a^{k_2} - E_a^{k_4}) \quad (3)$$

showing that e_{ss} can become temperature compensated when the sum of activation enthalpies in Eqn (3) becomes zero.

Rules for temperature-compensated and uncompensated flux in fixed networks

We now investigate the conditions for temperature compensation in simple reaction networks. The fluxes (reaction rates) can be characterized as input, internal and output fluxes (Fig. 2A). Under what conditions can a certain (output) flux (say J') become temperature compensated? In order to keep such an analysis tractable, the number of reaction intermediates is limited to four. In addition, input fluxes were limited to one with one or several output fluxes. An overview of the networks is shown in Fig. 2B,C. It may be noted that these networks do not represent a complete set of all possible networks containing four intermediates, but represent examples for which temperature compensation of flux J' becomes possible or not. However, based on these networks it is possible to derive some general rules (see below). For the sake of simplicity, we assume that the considered networks consist of first-order reactions (except when including feedback loops). In a metabolic context, this would reflect the view that under physiological conditions the enzymes that catalyze each reaction step are not saturated by their substrates [26]. Positive feedforward or feedback loops from an intermediate I to process i are described by replacing the original rate constant k_i with $k_i k [I]^n$, where k is an activation constant and n is the cooperativity (Hill coefficient). Negative feedback or feedforward loops from intermediate I to process i are described by replacing k_i with $k_i / (K_I + [I]^m)$, where K_I is an inhibitor constant and m is the cooperativity. For each network the steady-state output flux J' (indicated by the dashed box in each scheme) is examined in terms of whether temperature compensation is possible. The tested networks (supplementary Doc. S1) were then divided into those where J' is unable to exhibit temperature compensation (Fig. 2B) and those where J' can be compensated (Fig. 2C).

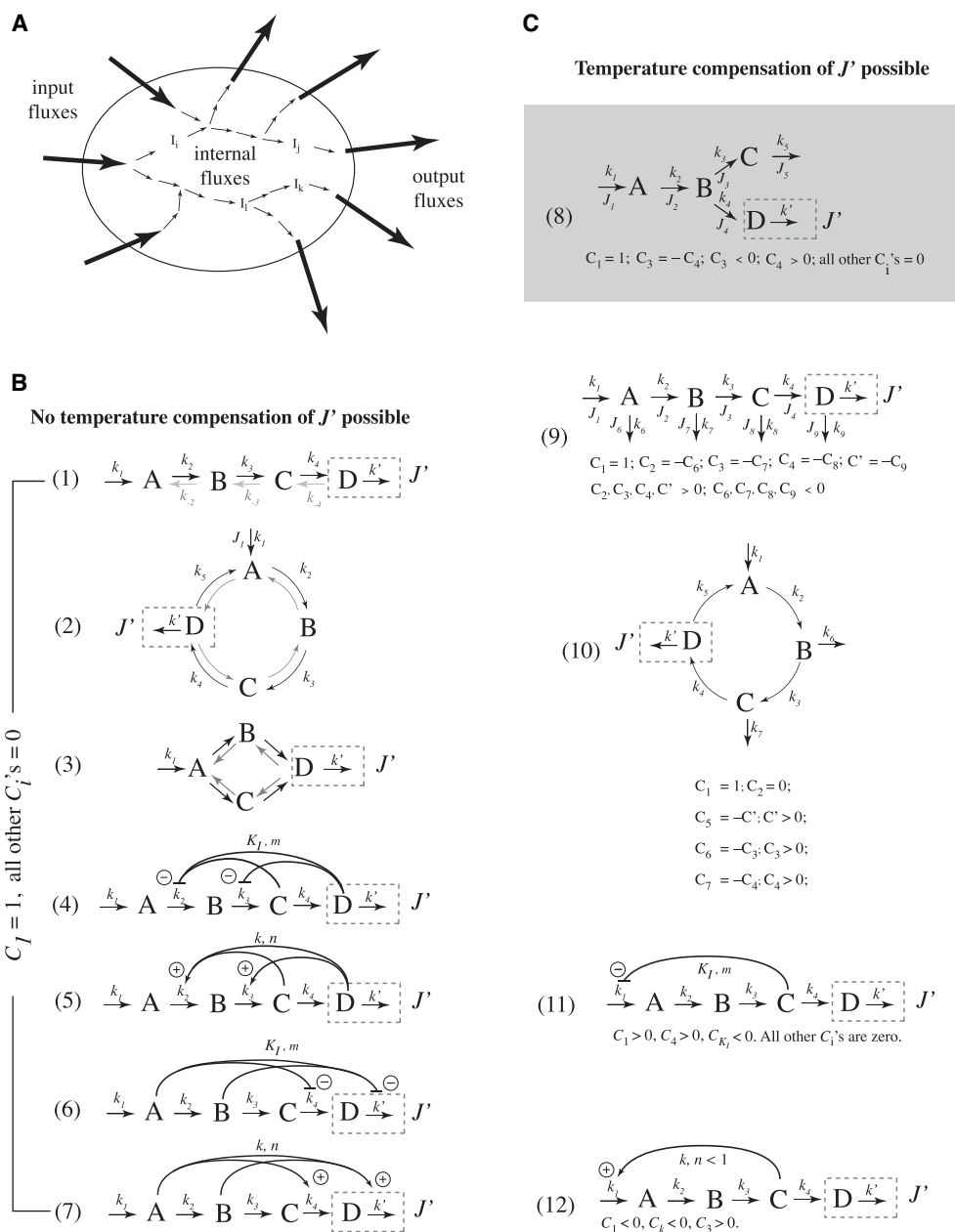


Fig. 2. Network models. (A) General scheme depicting input, internal and output fluxes. (B) Reaction schemes in which the steady-state flux J' cannot be temperature compensated. (C) Reaction schemes in which J' can be temperature compensated (see supplementary Doc. S1). For the sake of simplicity, global control coefficients (without an asterisk) are used and defined as $C_i = \frac{k_i}{J'} \left(\frac{\partial J'}{\partial k_i} \right)$, $C'_i = \frac{k'_i}{J'} \left(\frac{\partial J'}{\partial k'_i} \right)$, and $C_{K_i} = \frac{k_i}{J'} \left(\frac{\partial J'}{\partial K_i} \right)$, where k_i is the rate constant of reaction step i . Positive/negative signs indicate positive/negative feedforward or feedback loops leading to activation or inhibition of a particular process. For a description of the kinetics using activation constant k and inhibition constant K_i in positive or negative feedforward/feedback loops, see main text. Control coefficients with respect to k and K_i are defined as $C_k = \frac{k}{J'} \left(\frac{\partial J'}{\partial k} \right)$ and $C_{K_i} = \frac{k_i}{J'} \left(\frac{\partial J'}{\partial K_i} \right)$.

The following rules can be stated. Temperature compensation of an output flux is not possible for: (i) any (reversible or irreversible) chain or loop of (first-order) reactions or a branched network that has only one output flux and a product insensitive first step

(Fig. 2B, schemes 1–3); (ii) networks with only one output flux having in addition positive and/or negative feedback loops that are assigned to internal fluxes or to an output flux, but not to the first step (Fig. 2B, schemes 4–7). In all schemes of Fig. 2B $C_1 = 1$,

whereas all the other control coefficients are zero. Temperature compensation of an output flux becomes possible when: (i) the network has more than one output flux (Fig. 2C, schemes 8–10), or (ii) the networks have positive and/or negative feedback loops which are assigned to at least one input flux (Fig. 2C, schemes 11, 12).

From static to dynamic temperature compensation

In the derivation of Eqns (1a) and (1b) we assumed that activation enthalpies are constants and independent of temperature. Although this assumption is realistic for single-step elementary reactions, at the metabolic level of description activation enthalpies of enzyme-catalyzing steps may depend on temperature as enzymes may be affected by temperature-dependent processes such as phosphorylation, dephosphorylation and conformational changes. Because of these different levels of description we distinguish between static and dynamic temperature compensation. By static temperature compensation we mean that all activation enthalpies are assumed to be temperature independent and constant, and together fulfill the balancing equation for a certain reference temperature. To illustrate static and dynamic temperature compensation, as well as uncompensated behavior, we use scheme 8 (Fig. 2C) as an example. This scheme is one of the simplest models that can show temperature compensation of output flux J' . The control coefficients can be easily calculated (supplementary Doc. S1). We have taken a set of arbitrary rate constant values, and it may be noted that the behavior shown is not specific for the chosen rate constant values. Similar behavior can be obtained with any set of rate constants. Independent of the chosen rate constants, uncompensated behavior is obtained when all activation enthalpies are chosen to be equal, for example, E'_a . In this case, using the summation theorem $\sum_{i=1}^N C_i^J = 1$, Eqn (1a) can be expressed as $\frac{d \ln J'}{d \ln T} = \frac{E'_a}{RT}$, showing that flux J' is highly dependent on temperature. Such uncompensated behavior is shown in Fig. 3A (open squares) when all activation enthalpies in scheme 8 (Fig. 2C) are set to 67 kJ·mol⁻¹. In this case, J' shows an exponential increase with temperature. In Fig. 3B the increase in J' is seen when a 15 → 35 °C temperature step is applied to the uncompensated system. In static temperature compensation the activation enthalpies have been chosen such that Eqn (1a) is approximately fulfilled at T_{ref} (25 °C) at which the rate constants have been defined and the control coefficients have been evaluated (open diamonds, Fig. 3A). The condition for

static temperature compensation of scheme 8 reads: $E'_a k_1 + C_4^J (E_a^{k_4} - E_a^{k_3}) \cong 0$ with $C_4^J = \frac{k_3}{k_3 + k_4}$ (supplementary Doc. S1). Because the control coefficients depend on the rate constants and therefore on temperature, the static compensated flux J' will gradually change over an extended temperature range, as shown in Fig. 3A.

In dynamic compensation, one (or several) of the apparent (see above) or real activation enthalpies is allowed to change as a function of temperature. Processes that may lead to this include post-translational processing of proteins such as phosphorylation, dephosphorylation or conformational changes, and splice variation. [27,28]. For example, when $E_a^{k_1}$ increases with temperature as shown in the inset to Fig. 3A J' becomes practically independent of temperature (solid circles, Fig. 3A).

Incidentally, temperature compensation means that a steady-state flux (or the period length of an oscillatory flux, as for example in circadian rhythms) is (virtually) the same at different but *constant* temperatures. However, when a sudden change in temperature is applied, either as a step or as a pulse, even in temperature-compensated systems transient kinetics are observed, as illustrated in Fig. 3C. By applying a temperature step, J' undergoes an excursion and relaxes back to its steady state. The time scale of relaxation will be dependent on the rate constants, i.e. metabolic relaxation typically occurs in the subminute range. When gene expression adaptation is involved, relaxation may be much slower.

Figure 3D shows how in the static compensated case of Fig. 3A the various fluxes J_i depend on temperature. Although input flux J_1 increases exponentially with temperature ($J_1 = k_1 = A_1 e^{-\frac{E_1}{RT}}$), flux $J_4 = J'$ becomes compensated because J_3 (which also increases exponentially with temperature) removes just enough flux from J_1 (i.e. $J_4 = J_1 - J_3$) and thus ‘opposes’ or ‘balances’ J_1 's contribution to J_4 . In a static regulated network internal branching of the flux leading to two output fluxes may enable temperature compensation. There is experimental evidence for such a mechanism. For example in fish, the administration of [¹⁴C]glucose in the presence of citrate showed a dramatic increase in the [¹⁴C]lipid/¹⁴CO₂ ratio as a function of temperature, whereas carbon flow through the citric acid cycle was characterized by a Q_{10} of < 1 between 22 and 38 °C. This was attributed to an increased sensitivity of acetyl-CoA carboxylase to citrate activation at higher temperatures, resulting in elevated levels of fatty acid biosynthesis and a much lower than otherwise expected increase in carbon flow through the citric acid cycle [2,29].

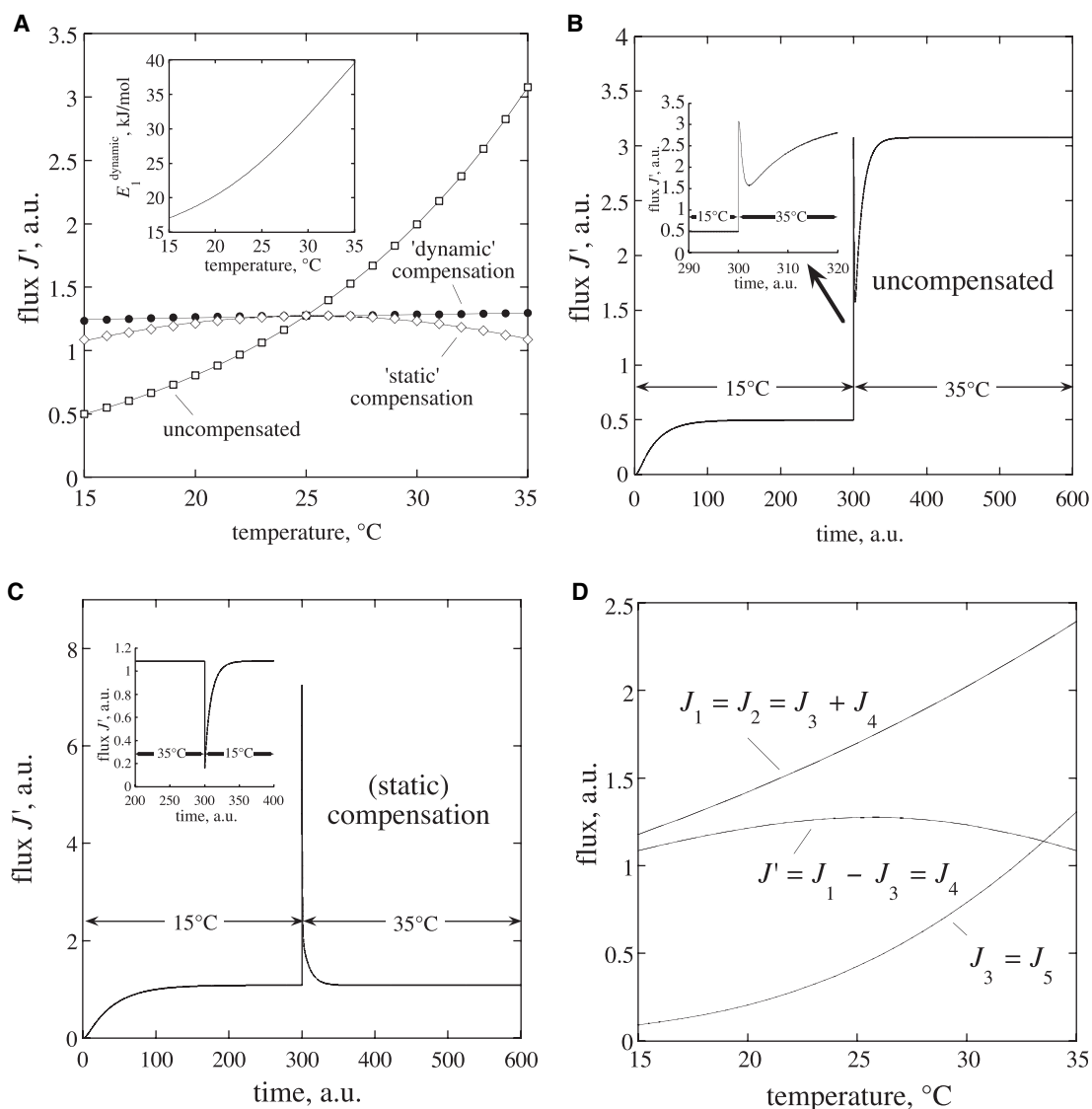


Fig. 3. Kinetics of compensated and uncompensated networks (8) (Fig. 2C). At 25 °C the rate constants have the following (arbitrary) values $k_1 = 1.7$ (time units) $^{-1}$, $k_2 = 0.1$ (time units) $^{-1}$, $k_3 = 0.5$ (time units) $^{-1}$, $k_4 = 1.5$ (time units) $^{-1}$, $k_5 = 1.35$ (time units) $^{-1}$, $k_6 = 0.7$ (time units) $^{-1}$. Initial concentrations of A, B, C, and D (at $t = 0$) are zero. The control coefficients (as defined in the legend of Fig. 2) at 25 °C are $C_1^J = 1.0$, $C_3^J = -0.250$, $C_4^J = 0.250$. (A) Open squares show the exponential increase of J' as a function of temperature for the uncompensated network (all activation enthalpies being taken 67 kJ·mol $^{-1}$; note: $E_a^{k_2}$, $E_a^{k_3}$ and $E_a^{k_6}$ do not matter, because the associated control coefficients are zero). Open diamonds show the effect of static temperature compensation of J' when using $E_a^{k_1} = 26$ kJ·mol $^{-1}$, $E_a^{k_3} = 120$ kJ·mol $^{-1}$ and $E_a^{k_4} = 22$ kJ·mol $^{-1}$. Solid circles show the effect of dynamic temperature compensation by keeping $E_a^{k_3}$ and $E_a^{k_4}$ constant but increasing $E_a^{k_1}$ (described as $E_1^{dynamic}$) with increasing temperatures as shown in the inset. For each temperature T $E_1^{dynamic}$ was estimated according to the equation $E_1^{dynamic}(T) = E_a^{k_1} - 0.5 \sum C_i^J(T) E_a^{k_i}$, where the $C_i(T)$ values were calculated at temperature T . (B) Transient kinetics of the uncompensated network (Fig. 3A) when applying a 15 \rightarrow 35 °C temperature step at $t = 300$ time units. The inset shows the details of the response kinetics. The difference in the J' steady-state levels at 15 and 35 °C is clearly seen. (C) Transient kinetics of the static temperature compensated network (Fig. 3A) when applying a 15 \rightarrow 35 °C temperature step at $t = 300$. The inset shows transient kinetics when a 35 \rightarrow 15 °C temperature step is applied. (D) Fluxes J_1 and J_3 as a function of temperature in the static temperature compensation of J' (Fig. 3A).

With an increasing number of output fluxes more output fluxes can be temperature compensated simultaneously. In scheme 9 (Fig. 2C), it is easy to see that J_6

can be compensated by J_2 , J_7 by J_3 , J_8 by J_4 and J' by J_9 . In the supplementary material a description is given how activation enthalpies can be found in order to

(statically) temperature compensate these output fluxes simultaneously.

Because at steady states internal fluxes are related to input and output fluxes, the above principles of how to temperature compensate one or several output fluxes can also be applied to internal fluxes. In networks with branch points (e.g. scheme 8, Fig. 2C), at least one of the downstream internal fluxes after the branch point can be temperature compensated, whereas none of the upstream fluxes can show temperature compensation unless there are more branch points upstream. The same applies also to cyclic networks. Testing, for example, the irreversible clockwise scheme 2 (Fig. 2B), fluxes J_2 , J_3 , J_4 and J_5 can be temperature compensated, whereas J_1 and J' cannot show temperature compensation.

Dynamic temperature compensation/adaptation in yeast

There is experimental evidence that dynamic temperature compensation occurs. As an example we show our experimental results obtained for yeast, but similar results have been reported for other organisms [30]. In Fig. 4, yeast cells were acclimated at three different temperatures (15, 22.5 and 30 °C) and overall metabolic rate (measured as the heat released from the cells) was determined as a function of temperature.

When cells that were adapted to 30 °C were cooled to 15 °C, a 4.6-fold decrease in metabolic rate was observed, suggesting the virtual absence of static temperature compensation. However, when the cells are allowed to acclimate at 15 °C, the decrease in flux is only 2.2-fold, indicating a substantial temperature compensation. As indicated above, this decrease in overall activation energy may be related to a variety of processes, such as altered gene expression or post-transcriptional modification of proteins/enzymes, but the mechanisms behind such adaptation are not well understood.

Temperature compensation in photosynthesis

Photosynthesis, the assimilation of CO_2 by plants, is a process that adapts to a plant's environment. Plants growing at low temperatures tend to have a relatively low but often temperature-compensated photosynthetic activity, whereas in plants living at high temperatures photosynthesis is uncompensated with a typical bell-shaped form. Figure 5A shows the photosynthetic rate (in terms of CO_2 uptake) for three plant species adapted to hot (*Tidestromia oblongifolia*), temperate (*Spartina anglica*) and cold (*Sesleria albicans*) thermal

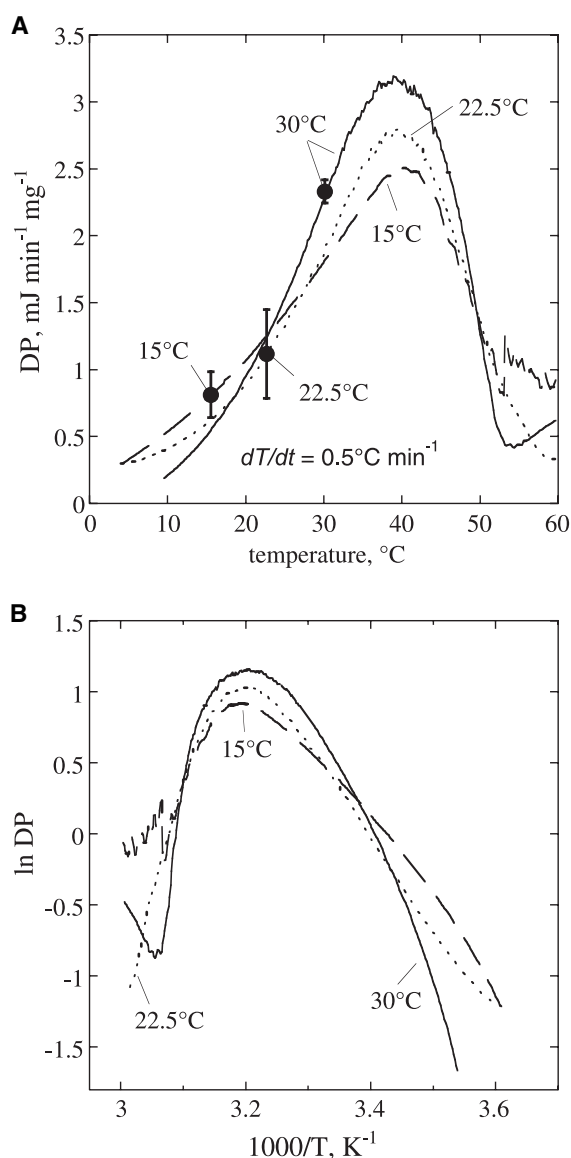


Fig. 4. Experimental evidence for dynamic temperature compensation. (A) Temperature-dependent metabolic activity of *S. cerevisiae*. The cells were acclimated at anaerobic conditions to 15, 22.5 and 30 °C. The anaerobic metabolic activity of the cells was measured as the overall generated differential power DP in $\text{mJ}\cdot\text{min}^{-1}$ per mg of wet cell biomass using differential scanning microcalorimetry ($0.5\text{ }^\circ\text{C}\cdot\text{min}^{-1}$). The curves are the average of $n = 4$ at 15 °C, $n = 16$ at 22.5 °C, and $n = 5$ at 30 °C. The large dots indicate metabolic activities at the corresponding acclimation temperatures with standard deviations. For temperatures $> 40\text{ }^\circ\text{C}$ the produced heat was lowered by cell death. (B) Arrhenius plots for the three acclimation temperatures. Activation enthalpies were estimated by linear regression between 4 °C (0.0036 K^{-1}) and 40 °C (0.0032 K^{-1}) for acclimation at 15 and 22.5 °C, and by linear regression between 10 °C (0.0035 K^{-1}) and 40 °C (0.0032 K^{-1}) for acclimation at 30 °C. Estimated activation enthalpies are: $44.8\text{ kJ}\cdot\text{mol}^{-1}$ (acclimation at 15 °C), $52.6\text{ kJ}\cdot\text{mol}^{-1}$ (acclimation at 22.5 °C), and $75.6\text{ kJ}\cdot\text{mol}^{-1}$ (acclimation at 30 °C).

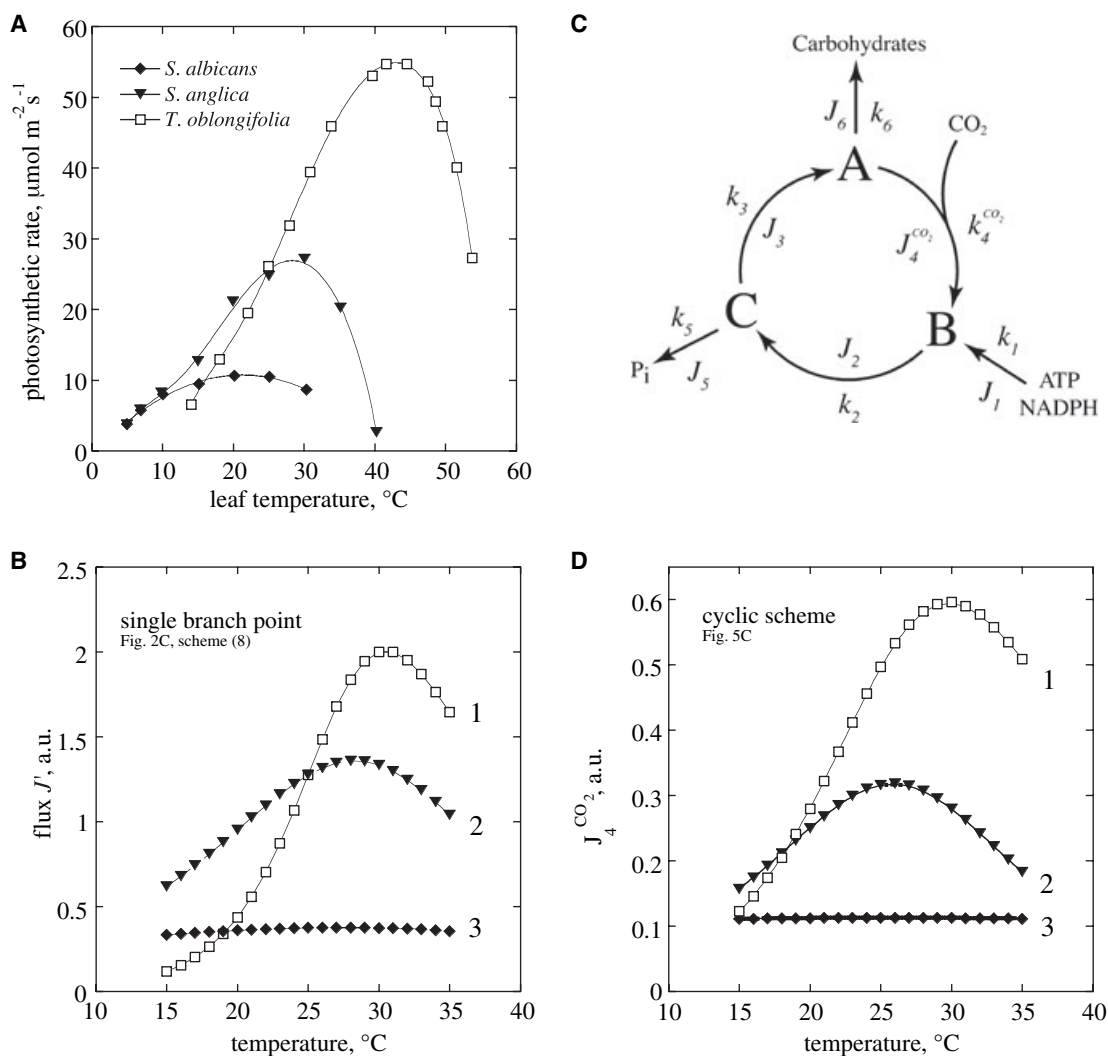


Fig. 5. Mimicking temperature compensation and temperature adaptation of photosynthesis in higher plants. (A) Photosynthetic flux of plant species living in hot (*S. albicans*), temperate (*S. anglica*) and cold environments (*T. oblongifolia*). Redrawn from Baker et al. [7]. (B) Temperature response of a single branch point (flux J_4 of scheme 8) with different activation enthalpy combinations. For the sake of simplicity, E_i are activation enthalpies for reaction step i with rate constant k_i . For details see supplementary Doc. S1. (1) $E_1 = 190 \text{ kJ}\cdot\text{mol}^{-1}$, $E_3 = 290 \text{ kJ}\cdot\text{mol}^{-1}$, $E_4 = 20 \text{ kJ}\cdot\text{mol}^{-1}$; (2) $E_1 = 70 \text{ kJ}\cdot\text{mol}^{-1}$, $E_3 = 190 \text{ kJ}\cdot\text{mol}^{-1}$, $E_4 = 20 \text{ kJ}\cdot\text{mol}^{-1}$; (3) $E_1 = 20 \text{ kJ}\cdot\text{mol}^{-1}$, $E_3 = 93 \text{ kJ}\cdot\text{mol}^{-1}$, $E_4 = 23 \text{ kJ}\cdot\text{mol}^{-1}$. In addition, the value of k_1 at $25 \text{ }^{\circ}\text{C}$ has been reduced from 1.7 to 0.5 (time units) $^{-1}$. All other rate constants and T_{ref} were as described in Fig. 3. (C) A minimal model of the Calvin Benson Cycle with reduction phase (fluxes J_1 , J_2 , J_5), regeneration phase (fluxes J_3 , J_6) and carbon dioxide assimilation (flux $J_4^{CO_2}$). (D) $J_4^{CO_2}$ as a function of temperature for three-parameter set combinations (curves 1–3). Joint rate constant values for all three curves (defined at $T_{ref} = 25 \text{ }^{\circ}\text{C}$): $k_2 = 0.1$ (time units) $^{-1}$, $k_3 = 0.5$ (time units) $^{-1}$, $k_4^{CO_2} = 1.5$ (time units) $^{-1}$ (concentration units) $^{-1}$ (concentration units) $^{-1}$, $k_5 = 1.35$ (time units) $^{-1}$, $k_6 = 0.7$ (time units) $^{-1}$. C_i values (at $T_{ref} = 25 \text{ }^{\circ}\text{C}$): $C_1 = 1$, $C_2 = 0$, $C_3 = -C_5 = 0.895$, $C_4 = -C_6 = 0.390$. k_1 values and activation enthalpy combinations: (1) $k_1 = 2.2$ (concentration units) (time units) $^{-1}$ $E_1 = 92 \text{ kJ}\cdot\text{mol}^{-1}$, $E_3 = 90 \text{ kJ}\cdot\text{mol}^{-1}$, $E_4 = 40 \text{ kJ}\cdot\text{mol}^{-1}$, $E_5 = 50 \text{ kJ}\cdot\text{mol}^{-1}$, $E_6 = 220 \text{ kJ}\cdot\text{mol}^{-1}$; (2) $k_1 = 1.4$ (concentration units) (time units) $^{-1}$ $E_1 = 62 \text{ kJ}\cdot\text{mol}^{-1}$, $E_3 = 70 \text{ kJ}\cdot\text{mol}^{-1}$, $E_4 = 40 \text{ kJ}\cdot\text{mol}^{-1}$, $E_5 = 50 \text{ kJ}\cdot\text{mol}^{-1}$, $E_6 = 220 \text{ kJ}\cdot\text{mol}^{-1}$; (3) $k_1 = 0.5$ (concentration units) (time units) $^{-1}$ $E_1 = 30.5 \text{ kJ}\cdot\text{mol}^{-1}$, $E_3 = 39 \text{ kJ}\cdot\text{mol}^{-1}$, $E_4 = 40 \text{ kJ}\cdot\text{mol}^{-1}$, $E_5 = 60 \text{ kJ}\cdot\text{mol}^{-1}$, $E_6 = 70 \text{ kJ}\cdot\text{mol}^{-1}$ with $\sum_{i=1}^6 C_i E_i = 0.012 \text{ kJ}\cdot\text{mol}^{-1}$. Note, because $C_2 = 0$, k_2 and activation enthalpy E_2 do not influence the steady-state value of $J_4^{CO_2}$ and its temperature profile. Also note, because $C_1 = 1$, $J_4^{CO_2}$ values can be changed by changing k_1 , but without changing the form of the temperature profile for $J_4^{CO_2}$.

environments [7]. Typically, the hot-adapted plant shows a relatively large variation in its photosynthetic response with a maximum at a relative high tempera-

ture, while the cold-adapted plant shows only a small variation in its photosynthetic response (temperature compensation). We have analyzed these temperature

responses in terms of a single branch point (because this is the simplest system that can show temperature compensation) and in terms of a 'minimal Calvin Benson cycle'.

Considering first the single branch point, analysis of scheme 8 (Fig. 2C) showed that the extent by which J_4 and J' become temperature compensated, mainly depends on the activation enthalpy for the influx J_1 and the activation enthalpy of the outflux J_3 , which 'competes with' the compensated flux $J_4 = J'$ for intermediate B. To obtain an uncompensated bell-shaped response (Fig. 5B, curve 1), activation enthalpies E_3 and E_4 need to be large. Reducing these activation enthalpies eventually leads to temperature compensation (Fig. 5B, curves 2, 3).

A more realistic model is shown in Fig. 5C, when the steady states of a simple representation of the Calvin Benson cycle are considered. This includes the balance between the input fluxes of ATP, NADPH and CO_2 , and the output fluxes of ADP, NADP^+ , P_i and carbohydrates [37]. A steady-state analysis of this model is given in the supplementary material showing that the assimilation of $\text{CO}_2 (J_4^{\text{CO}_2})$ can be temperature compensated, because of the balance of fluxes J_1, J_3, J_4 (positive contributions) with fluxes J_5 and J_6 (negative contributions). When the activation enthalpies of J_1 and J_3 dominate $J_4^{\text{CO}_2}$ shows the bell-shaped response for hot-adapted species (curve 1, Fig. 5D). Temperature compensation can be achieved when the positive contributions balance the negative, i.e. when the activation enthalpies of J_1 and J_3 are reduced (curve 3, Fig. 5D).

Conclusion

In this study we have derived a general relationship for how temperature compensation of a biochemical steady-state flux can occur by means of the balancing equations (Eqns 1a–c). Our focus was primarily how dynamic temperature compensation can occur via systems biology mechanisms [31]. The analysis shows that certain network topologies need to be met in order to obtain negative control coefficients. These negative control coefficients oppose the overall positive contributions of the control coefficients as indicated by the summation theorem $\sum_{i=1}^N *C_i^J = 1$ (or $\sum C_{k_i}^J = 1$ at the metabolic level). This can be achieved by various means: positive and negative feedforward and/or feedback loops, signal transduction events (e.g. by phosphorylation, dephosphorylation) and by adaptation through gene expression. As a special case of the derived principle, temperature compensation can occur for a single enzyme ('instantaneous temperature compensation') [2] when balancing occurs, for example, between the

enzyme's Michaelis–Menten constant (K_M, K_D) and its turnover number [32]. In this case, mechanisms that include enzyme–substrate interactions, enzyme modulator interactions, metabolic branch points, or conformational changes [2,27,28] may be involved. Although quantum mechanical tunneling is principally temperature independent, studies with methylamine dehydrogenase showed a strong temperature dependence of the enzyme-catalyzed process in which thermal activation or 'breathing' of the protein molecule is required to facilitate the tunneling reaction [33].

A challenge in applying realistic models is the description of how apparent activation enthalpies change with temperature and of the actual mechanisms involved in these processes.

Experimental procedures

Determination of yeast metabolic activities

Wild-type yeast strain *Saccharomyces cerevisiae* SPY509 (from the European *Saccharomyces cerevisiae* Archive of Functional Analysis; EUROSCARF, <http://web.uni-frankfurt.de/fb15/mikro/euroscarf/>) with genotype MAT or a, *his3Δ1*, *leu2Δ0*, *lys2Δ0*, *ura3Δ0* were grown in 250 mL flasks in 100 mL of complex YPD media (10 g yeast extract, 20 g peptone, and 20 g glucose in 1000 mL of the media) under constant nitrogen bubbling through the media and agitated at 250 r.p.m. at various acclimation temperatures [34,35]. Yeast cultures were always kept at the early exponential growth phase ($D_{660} < 2$) by diluting the culture with fresh media at each temperature. Acclimation time was at least 10–14 days. A differential scanning calorimeter (VP-DSC, MicroCal, Northampton, MA, USA) was used to measure heat production by living yeast. Yeast cells were washed in a 100 mM glucose solution (pH 5.5) at the relevant acclimation temperature under nitrogen bubbling to remove the YPD media, which has a high specific heat capacity, resuspended in 100 mM glucose solution to 10 g wet cell biomass per liter, and incubated at the acclimation temperature under a nitrogen atmosphere for 1 h before the measurements.

Before the measurements, all solutions were degassed, including the suspension of living cells. Glucose solution (100 mM) was used as the reference for the differential scanning calorimeter (DSC) measurements. The heat production was determined between 4 and 60 °C using a scanning rate of 0.5 °C·min⁻¹. Two independent sets of cells were scanned starting from the acclimation temperature either down to 4 °C or up to 60 °C. The heat production has been expressed in units of differential power (DP) per mg of wet cell biomass (mJ·min⁻¹·mg⁻¹). After each measurement, the yeast suspension was replaced with a freshly prepared one. About 80% of the metabolic activity of the yeast cells was estimated to correspond to anaerobic glycolysis.

Model calculations

Numerical calculations were performed using the FORTRAN subroutine LSODE (Livermore Solver of Ordinary Differential Equations) [36]. Some analytical solutions of steady-state fluxes were obtained with the help of MATLAB (<http://www.mathworks.com>).

Abbreviations and symbols

C_i , used in the supplementary material for $\frac{\partial \ln J_i}{\partial \ln k_i} = \frac{k_i}{J_i} \left(\frac{\partial J_i}{\partial k_i} \right)$.

* $C_i^{J_j}$, global control coefficient defined as $\frac{\partial \ln J_j}{\partial \ln k_i} = \frac{k_i}{J_j} \left(\frac{\partial J_j}{\partial k_i} \right)$.

$C_{k_i^{cat}}^{J_j}$, metabolic control coefficient defined as $\frac{\partial \ln J_j}{\partial \ln k_i^{cat}} = \frac{k_i^{cat}}{J_j} \left(\frac{\partial J_j}{\partial k_i^{cat}} \right)$.

e_i , concentration of enzyme which catalyzes process i .

e_{ss} , steady-state concentration of enzyme E in Fig. 1; see also Eqn (3).

E_i , abbreviation used in the supplementary material for $E_a^{k_i}$.

$E_a^{k_i}$, activation enthalpy of elementary component process with rate constant k_i . $E_a^{k_i}$ and k_i are related by the Arrhenius equation $k_i = A_i e^{-\frac{E_a^{k_i}}{RT}}$.

$E_a^{k_i^{cat}}$, activation enthalpy of turnover number k_i^{cat} of enzyme-catalyzed process i .

$E_a^{K_i}$, the formation enthalpy ΔH_i^0 of the rapid equilibrium between the enzyme and substrate in enzyme-catalyzed process i . The temperature dependence of K_i (or other equilibrium constants such as K_M , K_I) is analogous to the Arrhenius equation, i.e. $K_i = e^{-\frac{\Delta S_i^0}{R}} e^{-\frac{\Delta H_i^0}{RT}}$.

J_j , flux (reaction rate) of elementary component process j , or flux of enzyme catalyzed process j .

k , activation constant used in positive feedforward/feed-back loop.

k_i , rate constant of elementary component process i .

k_i^{cat} , turnover number of enzyme-catalyzed process i .

K_i , rapid equilibrium (dissociation) constant between enzyme and substrate in enzyme catalyzed process i .

K_I , inhibition constant used in negative feedforward/feed-back loop. For its temperature dependence, see also above description of $E_a^{K_i}$ and description of scheme 11 in the supplementary material.

K_M , Michaelis–Menten constant (Fig. 1).

m , used as an index for enzyme-catalyzed processes or to describe the cooperativity (Hill coefficient) in negative feedforward/feed-back loops acting from intermediate I on reaction i by replacing k_i with $k_i/(K_I + [I]^m)$.

n , cooperativity (Hill coefficient) in positive feedforward/feed-back loops acting from intermediate I on reaction i by replacing k_i with $k_i k [I]^n$.

R , gas constant.

$R_{T_i}^{e_m}$, metabolic response coefficient defined as $\frac{d \ln e_m}{d \ln T}$.

$R_{K_i}^{J_j}$, metabolic response coefficient defined as $\frac{d \ln J_j}{d \ln K_i}$.

* $R_{K_i}^{J_j}$, global response coefficient defined as $\frac{d \ln J_j}{d \ln K_i}$.

T , temperature.

T_{ref} , reference temperature at which rate constants and parameters are defined.

References

- Laidler KJ & Meiser JH (1995) *Physical Chemistry*, 2nd edn. Houghton Mifflin, Geneva, IL.
- Hazel JR & Prosser CL (1974) Molecular mechanisms of temperature compensation in poikilotherms. *Physiol Rev* **54**, 620–677.
- Zakhartsev MV, De Wachter B, Sartoris FJ, Portner HO & Blust R (2003) Thermal physiology of the common eelpout (*Zoarces viviparus*). *J Comp Physiol B* **173**, 365–378.
- Bünning E (1963) *The Physiological Clock*. Springer-Verlag, Berlin.
- Lloyd D & Murray DB (2005) Ultradian metronome: timekeeper for orchestration of cellular coherence. *Trends Biochem Sci* **30**, 373–377.
- Iwasaki K, Liu DW & Thomas JH (1995) Genes that control a temperature-compensated ultradian clock in *Caenorhabditis elegans*. *Proc Natl Acad Sci USA* **92**, 10317–10321.
- Baker NR, Long SP & Ort DR (1988) Photosynthesis and temperature, with particular reference to effects on quantum yield. *Symp Soc Exp Biol* **42**, 347–375.
- Cabrera HM, Rada F & Cavieres L (1998) Effects of temperature on photosynthesis of two morphologically contrasting plant species along an altitudinal gradient in the tropical high Andes. *Oecologia* **114**, 145–152.
- Pollheimer J, Zellner M, Eliassen MM, Roth E & Oehler R (2005) Increased susceptibility of glutamine-depleted monocytes to fever-range hyperthermia: the role of 70-kDa heat shock protein. *Ann Surg* **241**, 349–355.
- Peper A, Grimbergen CA, Spaan JA, Souren JE & van Wijk R (1998) A mathematical model of hsp70 regulation in the cell. *Int J Hyperthermia* **14**, 97–124.
- Hastings JW & Sweeney BM (1957) On the mechanism of temperature independence in a biological clock. *Proc Natl Acad Sci USA* **43**, 804–811.
- Ruoff P (1992) Introducing temperature compensation in any reaction kinetic oscillator model. *J Interdiscipl Cycle Res* **23**, 92–99.
- Ruoff P, Loros JJ & Dunlap JC (2005) The relationship between FRQ-protein stability and temperature compensation in the *Neurospora* circadian clock. *Proc Natl Acad Sci USA* **102**, 17681–17686.
- Kovács K, Hussami LL & Rábai G (2005) Temperature compensation in the oscillatory Bray reaction. *J Phys Chem A* **109**, 10302–10306.
- Kovács KM & Rábai G (2002) Temperature compensation in pH oscillators. *Phys Chem Chem Phys* **4**, 5265–5269.

- 16 Fell D (1997) *Understanding the Control of Metabolism*. Portland Press, London.
- 17 Heinrich R & Schuster S (1996) *The Regulation of Cellular Systems*. Chapman & Hall, New York, NY.
- 18 Kacser H & Burns JA (1973) The control of flux. *Symp Soc Exp Biol* **27**, 65–104.
- 19 Kahn D & Westerhoff HV (1991) Control theory of regulatory cascades. *J Theor Biol* **153**, 255–285.
- 20 Kell D & Westerhoff H (1986) Metabolic control theory: its role in microbiology and biotechnology. *FEMS Microbiol Rev* **39**, 305–320.
- 21 Westerhoff HV, Koster JG, Van Workum M & Rudd KE (1990) On the control of gene expression. *Control of Metabolic Processes* (Cornish-Bowden A, ed.), pp. 399–412. Plenum Press, New York, NY.
- 22 Cornish-Bowden A (2004) *Fundamentals of Enzyme Kinetics*, 3rd edn. Portland Press, London.
- 23 Brown GC, Westerhoff HV & Kholodenko BN (1996) Molecular control analysis: control within proteins and molecular processes. *J Theor Biol* **182**, 389–396.
- 24 Ruoff P, Christensen MK, Wolf J & Heinrich R (2003) Temperature dependency and temperature compensation in a model of yeast glycolytic oscillations. *Biophys Chem* **106**, 179–192.
- 25 Chen Y & Westerhoff HV (1986) How do inhibitors and modifiers of individual enzymes affect steady-state fluxes and concentrations in metabolic systems? *Math Model* **7**, 1173–1180.
- 26 Dixon M, Webb EC, Thorne CJR & Tipton KF (1979) *Enzymes*. Longman, London.
- 27 Hochachka PW & Somero GN (2002) *Biochemical Adaptation. Mechanism and Process in Physiological Evolution*. Oxford University Press, Oxford.
- 28 Somero GN (1995) Proteins and temperature. *Annu Rev Physiol* **57**, 43–68.
- 29 Hochachka PW (1968) Action of temperature on branch points in glucose and acetate metabolism. *Comp Biochem Physiol* **25**, 107–118.
- 30 Hikosaka K, Ishikawa K, Borjigidai A, Muller O & Onoda Y (2006) Temperature acclimation of photosynthesis: mechanisms involved in the changes in temperature dependence of photosynthetic rate. *J Exp Bot* **57**, 291–302.
- 31 Alberghina L. & Westerhoff HV (2006) *Systems Biology. Definitions and Perspectives*. Springer-Verlag, Berlin.
- 32 Andjus RK, Dzakula Z, Marjanovic M & Zivadinovic D (2002) Kinetic properties of the enzyme–substrate system: a basis for immediate temperature compensation. *J Theor Biol* **217**, 33–46.
- 33 Sutcliffe MJ & Scrutton NS (2000) Enzyme catalysis: over the barrier or through the barrier? *Trends Biochem Sci* **25**, 405–408.
- 34 Burke D, Dawson D & Stearns T (2000) *Methods in Yeast Genetics. A Cold Spring Harbor Laboratory Course Manual*. Cold Spring Harbor Laboratory Press, Cold Spring Harbor, NY.
- 35 Sambrook J, Fritsch EF & Maniatis T (1989) *Molecular Cloning: A Laboratory Manual*. Cold Spring Harbor Laboratory Press, Cold Spring Harbor, NY.
- 36 Radhakrishnan K & Hindmarsh AC (1993) *Description and Use of LSODE, the Livermore Solver for Ordinary Differential Equations. NASA Reference Publication 1327*. Lawrence Livermore National Laboratory Report UCRL-ID-113855. National Aeronautics and Space Administration, Lewis Research Center, Cleveland, OH.
- 37 Horton HR, Moran LA, Scrimgeour KG, Perry MD & Pearson RJ (2006) *Principles of Biochemistry*. Prentice Hall, Upper Saddle River, NJ.

Supplementary material

The following supplementary material is available online:

Doc. S1. Derivation of Eqns 1a and 1b; analysis of reaction schemes in Fig. 2B,C, and analysis of the Calvin Benson cycle of Fig. 5C.

This material is available as part of the online article from <http://www.blackwell-synergy.com>

Please note: Blackwell Publishing is not responsible for the content or functionality of any supplementary materials supplied by the authors. Any queries (other than missing material) should be directed to the corresponding author for the article.